Sensors and Actuators B 178 (2013) 132–139

Contents lists available at SciVerse ScienceDirect

Sensors and Actuators B: Chemical

journal homepage: www.elsevier.com/locate/snb

Charge transfer and stability of implantable electrodes on flexible substrate

M.M.R. Howlader[a,*], T.E. Doyle[a], S. Mohtashami[a], J.R. Kish[b]

[a] Department of Electrical and Computer Engineering, McMaster University, Hamilton, Ontario L8S 4K1, Canada
[b] Department of Materials Science and Engineering, McMaster University, Hamilton, Ontario L8S 4L8, Canada

ARTICLE INFO

Article history:
Received 15 August 2012
Received in revised form 5 December 2012
Accepted 14 December 2012
Available online xxx

Keywords:
Electrochemical impedance
Surface roughness
Liquid crystal polymer
Charge transfer
Implantable electrodes
Neuromuscular stimulation

ABSTRACT

Beyond their biocompatibility, implanted electrodes for neuromuscular stimulation require careful consideration of conductivity, stability, and charge delivery capacity (CDC) to avoid irreversible faradaic reactions. To study these requirements, metal electrodes of platinum (Pt), gold (Au), and titanium (Ti) on flexible liquid crystal polymer are fabricated using electron-beam evaporation, and investigated by electrochemical impedance spectroscopy, cyclic voltammetry and atomic force microscopy. A theoretical model is used to explain the physical functionalities. Frequency dependent electrochemical interfacial impedance is observed. The impedance as well as long-term electrochemical stability is influenced by the surface roughness, reactivity and capacitance of the electrodes. Pt electrode offers lower impedance in the neuromuscular stimulation frequencies and higher CDC than that of Ti and Au, but is not as stable as Au electrode.

1. Introduction

Implanted electrodes for neuromuscular stimulation provide better specificity and enhanced control over transcutaneous or percutaneous excitation [1–5]. The advances in prostheses do not offer an advantage to a subject that has retained the affected limb(s). Rather than an orthosis, an implanted electrode may offer a better alternative rehabilitative solution. However, an implanted electrode must maintain biocompatibility while offering optimum stable charge transfer [6].

Recent works on the electrode/electrolyte interface have been investigated through flexible polymer substrate with various electrode metal layers for improved implantation characteristics [1,3,6]. The characteristics of double layer capacitive reactions and reversible faradaic charge transfer reactions are fundamental to the implanted electrode. The amount of charge required for metal electrodes to reach the necessary activation can greatly exceed ideal capacitive transfer. Therefore, it is essential to determine the reversible charge injection limit [2,7]. Compared to rigid substrates, flexible ones provide a safer excitation by moving with nerves. Flexible substrates do not apply compression on the nerves and minimize abrasion from relative movement of the nerves and electrode. Flexibility also enhances mechanical fixation which better maintain the ideal charge transfer at electrode/tissue interface. Preference of such flexibility leads the electrodes material technology (substrate and conductor) toward using biocompatible polymers as electrodes substrates [1]. Polyimide (PI) is a common flexible substrate in electrical stimulation electrodes [1,7–10]; however, it has high water absorption via the adhesion layer/polyimide interface and is thus subject to hydrolytic attack and delamination [11]. Compared to PI, liquid crystal polymer (LCP) substrate offers lower water absorption [11] and enhances the long-term electrochemical stability of electrodes. The authors present the seminal work on the usage of LCP as the biocompatible flexible substrate [12] for the application of implanted electrodes.

Beyond biocompatibility and flexibility, implanted electrodes should transfer maximum electrical impulse at lowest injected charge. This requires lowest possible impedance. The electrodes are also required to provide charge delivery capability that avoids the harmful chemical changes in both tissue fluid and electrodes. To study the effect of different electrode materials, the authors chose the commonly used gold (Au), platinum (Pt), and titanium (Ti) with flexible substrate. Further, the effects of elapsing time on the electrochemical performance of implanted electrodes with different materials and deposition techniques need to be evaluated. Based on a study of long-term electrical behavior of 16 different electrode materials using electrochemical interfacial impedance measurements for 10 days, an increase in impedance for all materials was observed over the first days [13]. After the initial increase of impedance for the electrodes with polarizable metals such as Pt, Au and Iridium (Ir), the impedance stayed almost constant for 1 week. However, [13] reported decrease in impedance with progressing time for some materials, such as

* Corresponding author. Tel.: +1 905 525 9140x26647; fax: +1 905 521 2922.
E-mail address: mrhowlader@ece.mcmaster.ca (M.M.R. Howlader).

0925-4005/$ – see front matter © 2012 Elsevier B.V. All rights reserved.
http://dx.doi.org/10.1016/j.snb.2012.12.051

silver, carbon and doped tin oxide. On the other hand, the double layer parameters have been investigated for different materials such as aluminum (Al), Au, Ti, and magnesium (Mg) alloy in diverse moles of electrolytes [8,14–16]. Diversity in the electrodes, substrate materials, and electrolytes (e.g., phosphate buffered saline vs. sodium sulfate) results in dispersive double layer behavior. The double layer dispersion has been discussed on the literature using surface roughness, reactivity and adhesion, inhomogeneity, oxidation, porosity, and geometry of electrode [13–18]. For example, the electrochemical impedance behavior of uncoated orthopedic surgical implant Ti–6Al–4 V (vanadium) alloys in a solution of sodium chloride, calcium chloride and potassium chloride with compositions of 8.6, 0.48, and 0.3 gdm^{-3}, respectively showed formation of a few tens of nanometer thick porous oxide film [16].

To investigate the electrochemical characteristics of the presented polymer–metal electrodes, the authors present electrochemical measurements of Au, Ti, and Pt deposited electrodes on LCP immersed in phosphate buffered saline (PBS) solution [5,8,9]. To determine the best polymer–metal electrode for long term implantation, an extended electrode analysis was conducted with the measurements of root mean square (RMS) surface roughness, and electrochemical impedance of the electrode/electrolyte interface. In addition, the long term impedance was compared against the equivalent circuit model, and cyclic voltammograms were performed to determine charge delivery capacity (CDC).

2. Experimental procedure

In this research, Au, Pt, and Ti were the electrode electroactive portion with thickness of 200 nm. To enhance the adhesion a 30 nm Ti layer was deposited between the conducting layer and LCP. The substrate specimens were cut from an A4 size LCP sheet. A 100 μm thick copper deposition mask was prepared with 8 mm diameter and placed on the LCP. Adhesion and conducting layers were deposited through electron beam evaporation at 1.5 Angstroms/s with background pressure of 1E−4 Pa. The deposition conditions such as target location, sample location, parameters for target, chamber conditions were kept constant for all electrodes. Prepared electrodes were investigated using atomic force microscope (AFM-ICON from Veeco) and electrochemical Gamry framework workstation. The latter instrument provides electrochemical impedance spectroscopy (EIS) and cyclic voltammetry (CV). The EIS and CV measurements were performed at room temperature in 0.1-M phosphate buffered saline (PBS) solution. PBS is a saline solution containing sodium chloride, sodium phosphate, potassium phosphate and potassium chloride, and is commonly used as the physiological medium in biological research.

Fig. 1 shows a schematic of the electrochemical measurement apparatus and the equivalent circuit model of the electrode/electrolyte interface. The model consists of a capacitive interface with constant phase element (CPE) described by the double layer, in parallel with a charge transfer resistance (R_{ct}), in series with the electrolyte resistance (R_e). CPE impedance is given by [8,13,14]:

$$Z_{CPE} = \frac{1}{K(j\omega)^{\beta}}, \quad (1)$$

where K is the numerical value of the admittance at $\omega = 1$ rad s^{-1}, j is the imaginary number ($j = \sqrt{-1}$), ω is the angular frequency ($\omega = 2\pi f$, f being the frequency), and β a value (0–1) indicating the deviation from a pure ($\beta = 1$) capacitance. The surface and volume resistivities of the LCP are 1E14 Ohm and 1E13 Ohm m, respectively.

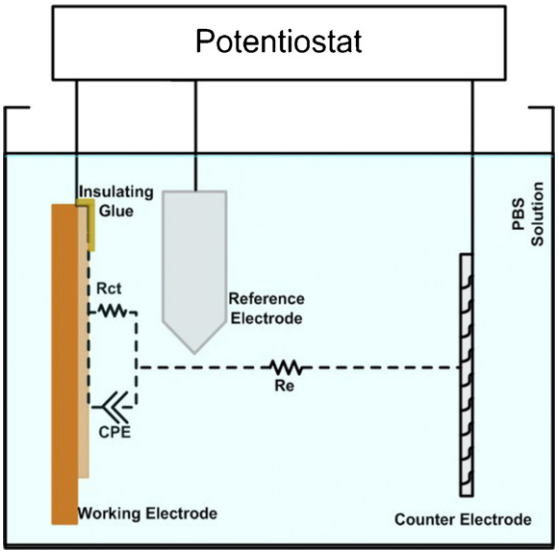

Fig. 1. Schematic for electrochemical measurements with equivalent circuit model of electrode/electrolyte interface.

Thus, the influence of current through LCP is negligible compared to the parallel metal electrodes.

For studying stability of the electrodes, each electrode was immersed in PBS solution for 42 days at room temperature. Through this 42-day period, electrodes underwent electrochemical impedance spectroscopy measurements at 3, 7, 14, 21, 28, 35, and 42 days. Upon conclusion of EIS measurements, RMS surface roughness of electrodes were observed and compared with their original values.

The electrochemical impedance spectra of these metals are analyzed in terms of the exponent of CPE impedance, characteristic behavior of capacitance, the numerical value of admittance, and charge transfer resistance. These parameters were determined using a nonlinear least-squares curve fitting of experimental data from ZView software.

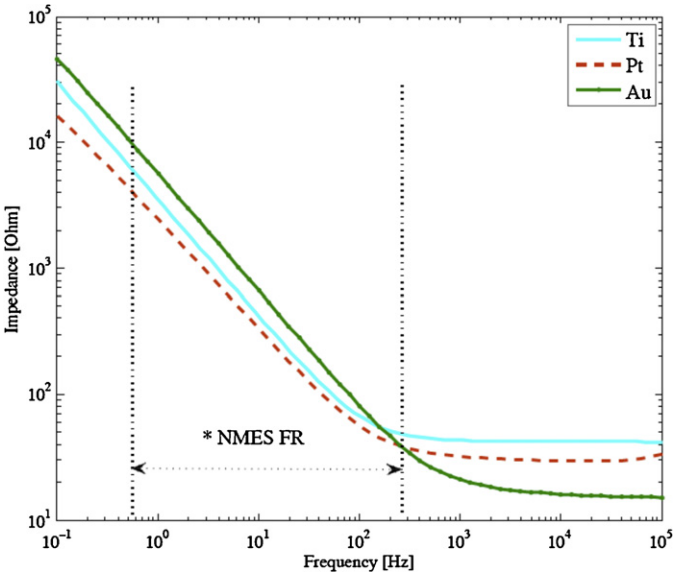

Fig. 2. Electrochemical interfacial impedance of Pt, Au and Ti electrodes of 8 mm diameter surface area as a function of frequency. Note NMESFR stands for neuromuscular electrical stimulation frequency range.

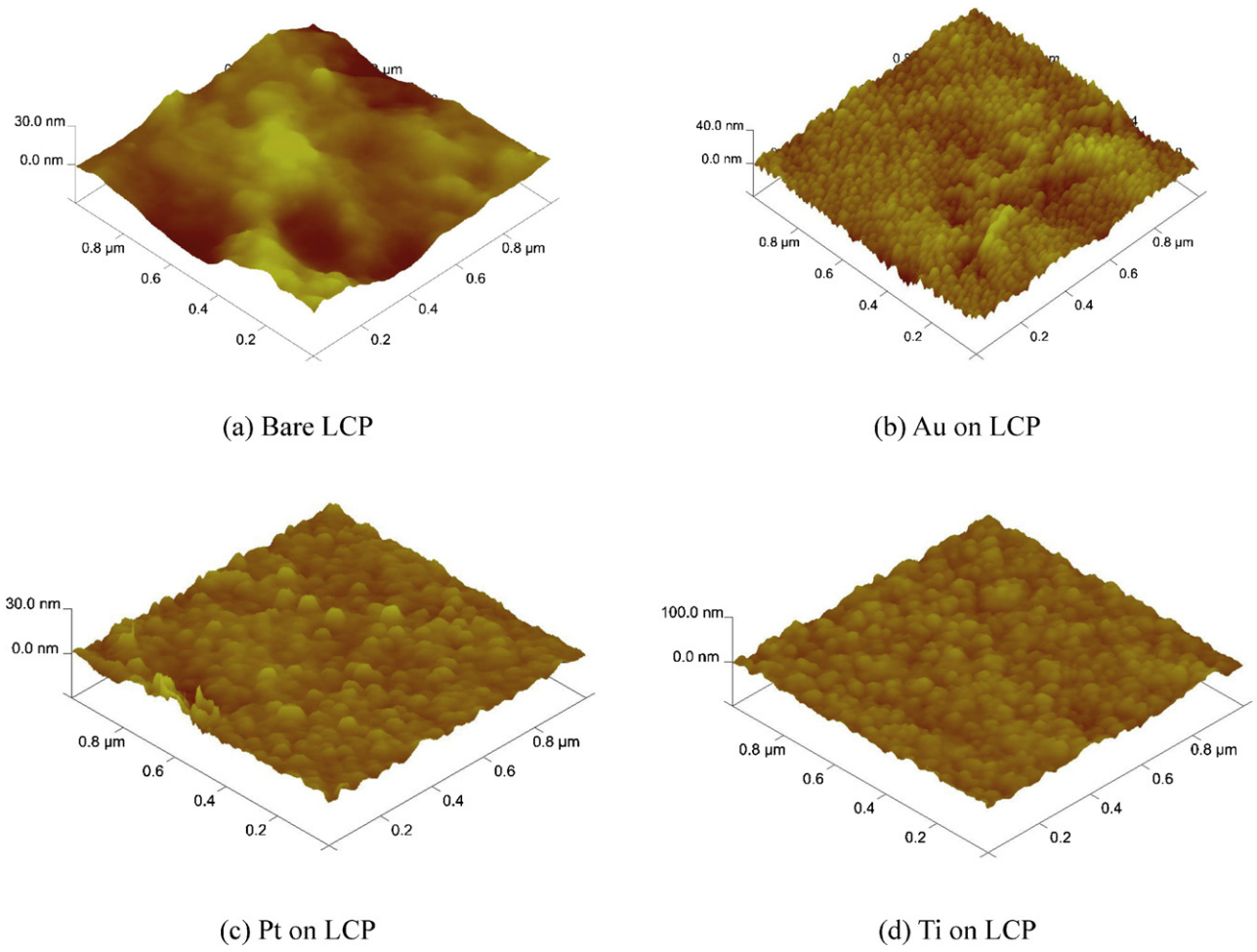

Fig. 3. Three-dimensional AFM images of LCP (a) bare substrate, (b) with deposited Au (c) with deposited Pt, and (d) with deposited Ti electrodes from a 1 μm × 1 μm area.

3. Results and discussion

3.1. Electrochemical interfacial impedance dependence on frequency

Fig. 2 shows the electrochemical interfacial impedances of Pt, Au and Ti electrodes as a function of frequency. Hereafter, we refer to electrochemical interfacial impedance as impedance. The impedance of the electrodes increases with the decrease of frequency. Significant differences in the impedance of the electrode materials in the measured frequency range are observed. Lower impedance requires lower amount of injected charge to transfer certain electrical impulse and hence is desired. If we consider the neuromuscular electrical stimulation frequency range (NMES FR), it is observed from Fig. 2 that the order in the impedance changes at the defined cut-off intercept of rising slope tangent with the lines of constant impedance. The cut-off frequency can be expressed by the following equation.

$$f_c = \frac{1}{2\pi R_e K} \quad (2)$$

where K is defined in Eq. (1), and describes the double layer capacitance involving charge transfer ability of the electrode to electrolyte (body tissue) [8,13,14,19].

At high frequency, Ti electrode shows highest impedance followed by Pt and Au. While the impedance for Ti and Pt remains almost constant to the cut-off frequency, it gradually increases for Au with the decrease of frequency. CPE approximates a short circuit at high frequency, resulting in R_{ct} to be neglected and the system to function as a high-pass filter with the cut off frequency.

Through cut-off frequency to the lower frequency range, Au electrode shows highest impedance followed by Ti and Pt. At low frequency, CPE becomes an open circuit, resulting in an equivalent impedance of $R_e + R_{ct}$. Therefore, the variation in the impedance at low frequency range is due to the small changes in R_e, and experimental uncertainties, i.e., change in ambient.

An electrode with a rougher surface exhibits a larger surface area, thus the numerical value of CPE (i.e., K) increases with increase of surface roughness making its value proportional to the surface area. The implication is that, in short-term, an electrode with a rougher surface should exhibit a lower cut-off frequency. From Fig. 2 we observe that in fact, the cut-off frequency of Ti electrode was lower than that of Pt and Au. Therefore, surface roughness of the electrode material influences the impedance and relevance to the deviation of constant phase element double layer from pure capacitive behavior.

3.2. Surface roughness vs. impedance

We have comprehensively investigated the surface roughness to explain its role in interfacial electrochemical impedance. Fig. 3 illustrates the three-dimensional AFM images of (a) bare LCP and (b) Au, (c) Pt and (d) Ti deposited on LCP substrates from scanning a 1 μm × 1 μm area. The RMS surface roughness of bare LCP is 4.6 nm. After deposition under identical conditions, the roughness of Au, Pt and Ti electrode on LCP was 3.18, 3.44, and 4.49 nm, respectively. A

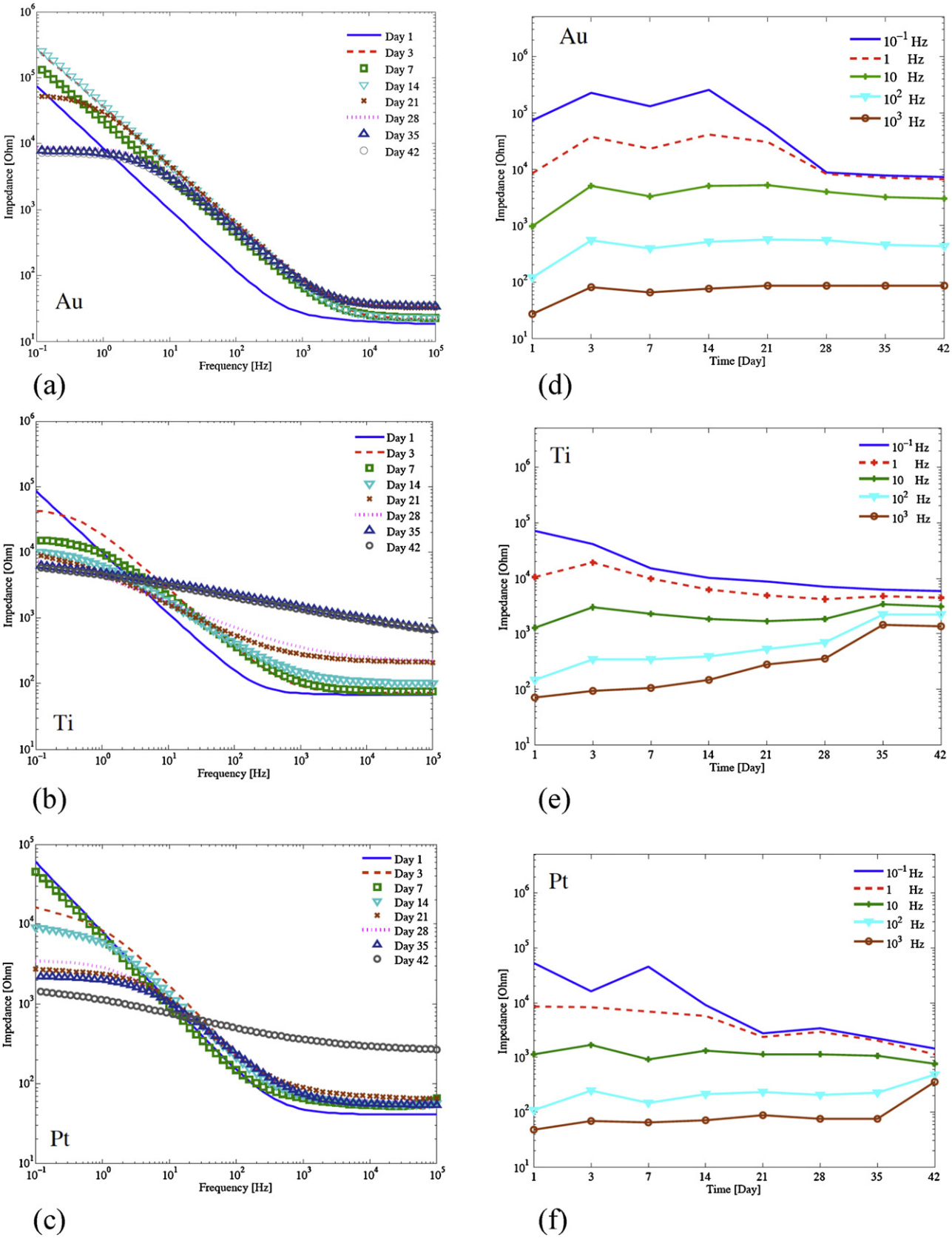

Fig. 4. Electrochemical impedance spectra of Au, Ti and Pt electrodes through the 42-day experiments as a function of frequency (a–c), and as a function of elapsed time at 10^{-1}, 1, 10, 10^2 and 10^3 Hz (d–f).

Table 1
Electrode/electrolyte interface model parameters changing through 42 days of immersing electrodes in PBS solution obtained from fitting experimental data to model. RMS surface roughness of a 1 μm × 1 μm scan area of electrode on LCP before and after the 42-day experiments.

Days	Au				Pt				Ti			
	K ($\times 10^{-5}$)	β	R_{ct}(kΩ)	RMS surf. rough. (nm)	K ($\times 10^{-5}$)	β	R_{ct} (kΩ)	RMS surf. rough. (nm)	K ($\times 10^{-5}$)	β	R_{ct} (kΩ)	RMS surf. rough. (nm)
1	1.8	0.83	1200	3.18	21	0.88	2700	3.44	22	0.93	3600	4.49
3	5.4	0.84	1100	–	1.18	0.84	16	–	0.9	0.89	46	–
7	0.94	0.86	1000	–	2.11	0.84	13.4	–	1.6	0.81	16.5	–
14	0.42	0.92	849	–	2.32	0.84	9.5	–	2	0.7	11.8	–
21	0.5	0.9	55	–	2.78	0.8	3.4	–	5.2	0.6	11.7	–
28	0.59	0.88	8.8	–	3.3	0.78	3	–	7	0.5	11	–
35	0.8	0.86	7.8	–	2.9	0.78	2.1	–	8.2	0.25	10.5	–
42	0.9	0.85	7	11	2.8	0.38	1.6	NA[a]	9.6	0.25	10.5	6.03

[a] NA that surface roughness of Pt on LCP was not measurable due to delamination.

comparison between the roughness of the bare LCP substrate and the Au, Pt and Ti deposited electrodes on LCP shows a 30% decrease, a 25% decrease and an almost 0% change, respectively. This indicates that the electrode materials smoothens LCP surface. Au electrode offers the smoothest surface followed by Pt and Ti. In the selected neuromuscular stimulation frequency range of 1–250 Hz, Au with the lowest RMS surface roughness presents the highest f_c producing the highest electrochemical impedance, followed by Ti and Pt. An increase in surface roughness will increase the true surface area, resulting in increased double layer capacitance and therefore decreasing the impedance of the constant phase element.

3.3. Impedance stability vs. frequency and time

Fig. 4 shows the electrochemical impedance spectra of Au, Ti and Pt electrodes through the 42-day experiments (a, b, c are plotted against frequency for specific times and d, e, f are plotted against time for specific frequencies). Observing Fig. 4a–c, the impedance was increased on the third day, then decreased on the 14th day compared to the previous measurement and finally increased significantly after 42 days. The slope of impedance spectra was changed at the cut-off frequency and reduced with the increase in the immersion time of the electrodes. However, Au electrode shows more consistency in keeping the slope of its impedance spectra close to one. The slope decrease is a result of a drop in β value. Considering Eq. (2), this drop in β value is a result of the diversion of double layer's capacitive behavior. It offers that with elapsing time, surface roughness increases due to water absorption. This increase of surface roughness is likely to cause R_{ct} to decrease. Therefore, the long-term impedance results in higher cut-off frequencies for the electrodes with increased surface roughness which is in contrast to that of short-term.

Fig. 4d–f shows the immersion time dependent electrochemical impedance of Au, Ti and Pt in the frequencies of interest in PBS. At low frequencies (i.e., 10^{-1} and 1 Hz), the impedance for all the electrodes shows negative slope with respect to the immersion time. Above these frequencies (i.e., 10^1, 10^2 and 10^3 Hz), for Au we observe near independence of impedance and immersion. For Ti the impedance increases with immersion. This increase is attributed to the hydrolytic attack of the Ti, which may have been covered by a TiO_2 layer (which is hydrophilic) due to atmospheric exposure, prior to PBS immersion [20]. In the case of Pt, at 35 days, the impedance transitions from independent to an unexpected dependence and increase; we believe this a residual result of prior delamination.

Table 1 demonstrates circuit model parameters during the 42-day stability experiments. Each electrode type surface roughness increases with time due to water absorption causing the model R_{ct} to decrease. The increase in the RMS surface roughness increases the double layer capacitance but decreases the cut-off frequency. A significant drop in β for both Pt and Ti is observed in long-term evaluation. The decreases in R_{ct} and β values, and the changes in K value, are due to the change in capacitive and faradaic behaviors in long-term studies [15]. However, Au electrodes offer β-unchanged values, close to one, after 42 days of immersion into the PBS solution. This is indicative of best stability of Au electrodes due to reversible capacitive reactions. Optical images for Au (not shown due to similar behavior of Ti) and Ti electrodes after 42 days

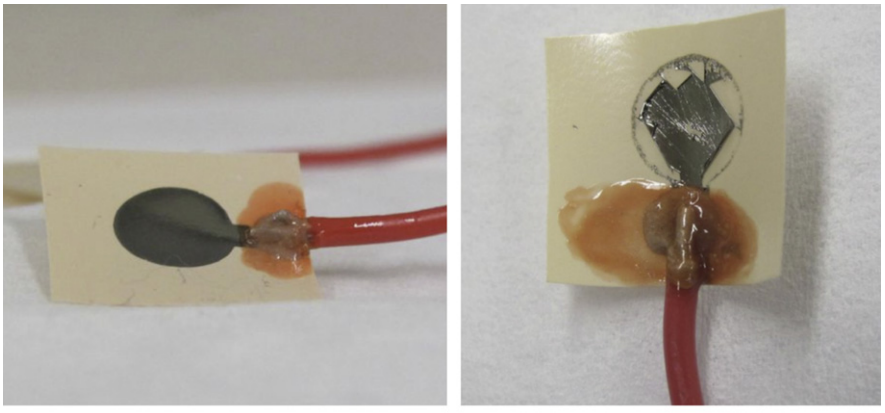

(a) Ti (b) Pt

Fig. 5. Optical images for (a) Ti and (b) Pt electrodes after 42 days. Ti and Pt electrodes show no delamination and delamination, respectively.

Table 2
Calculated CDC values from CV curves of deposited electrodes at 1E-4 Pa in this study compared to their values from literature.

Film	CDC value (mC cm^{-2})	
	This study	Literature
Pt	3.12	2.92–26.8[1], 4.4[24]
Au	0.33	0.24[26]
Ti	0.20	0.59[25]

showed no delamination (Fig. 5a). In contrast, delamination of Pt electrode after 42 days of immersion into the PBS solution was observed (Fig. 5b). Pt, due to its hydrophilic nature, is more prone to hydrolytic attack from the saline solution (PBS), compared to Au and Ti (which are hydrophobic) [21,22]. Therefore, the stability study shows that Au and Ti electrodes on LCP have potentials for long-term applications over Pt.

The reduction of β with elapsing time was observed due to rough surface. Identical to these observations, from Table 1, an increase in surface roughness and a decrease in β of Ti and Pt electrode after elapsing time in PBS electrolyte have been observed in our study. In other study [16], current densities of titanium alloys were measured in saline solution of 0.9% NaCl in compared with pure Ti. Lower values of current densities of Ti alloys than pure Ti were observed to be due to the formation of passive film (oxide) with time. The passivated film [23] resulted in the increase of the resistance of the Ti alloys. Therefore, the characteristic parameters of CPE significantly control the distributions of current and potential, and ultimately the electrochemical interfacial impedance of electrode/electrolyte.

For Au, the surface roughness was significantly increased after elapsing time and is comparable to that of Ti. The K value was relatively lower compared to that of Ti. While the β for Au remained constant, it was severely decreased in Pt and Ti. The significant decrease observed for Ti may be explained by the formation of a more porous outer oxide surface layer with extended exposure time. The addition of H_2O_2 to PBS solution has been found to significantly reduce electrochemical performance, β value in particular, of Ti [15,22,23]. The degraded electrochemical performance is attributed to the formation of rougher, more porous, oxides with increased ionic conductivity in the presence of H_2O_2. However, the exact mechanism by which this occurred in the experimental conditions employed herein is not known, and requires further study. Identical electrochemical behavior of Pt to that of Ti is likely attributed to the applied potential induced oxidation behavior [17,18] associated with delamination of Pt. Hence, the increase in the surface roughness associated with oxidation and porosity is responsible for the poorly dependent electrochemical impedance behavior of Ti and Pt as a function of frequency in the stability test. Conclusively, the chemical environment on the surface and inside the electrode (i.e., pores) controls changes in the electrochemical interfacial impedance of electrode/electrolyte with the time elapsed immersion of Ti and Pt in the electrolyte.

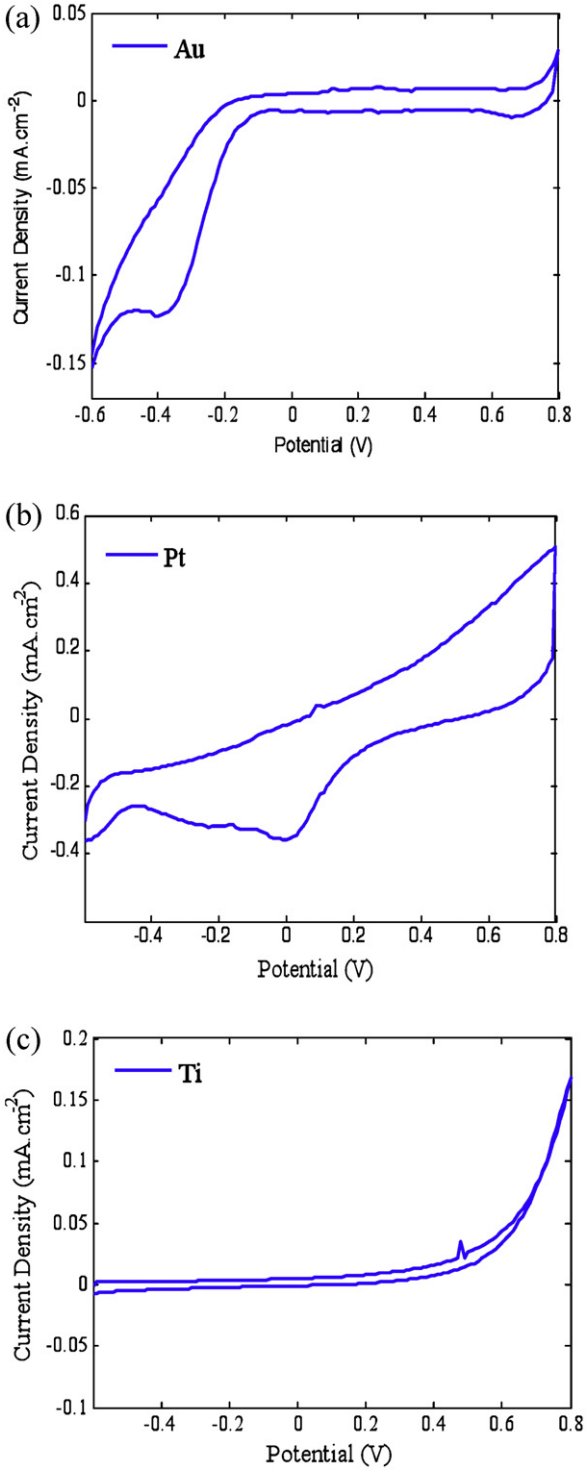

Fig. 6. Cyclic voltammograms of (a) Au, (b) Pt and (c) Ti. The area inside each curve is CDC value.

3.4. Charge delivery capacity

Cyclic voltammograms (100 mV/s) of Pt, Au, and Ti electrodes were performed to evaluate the ability of each electrode type to convert electrical current into ionic current at electrode's surface and vice versa through calculating the charge delivery capacity (CDC – obtained by measuring the enclosed area inside the cyclic voltammogram graph) over the range of −0.6 V to 0.8 V. Voltage sweep is limited to this range to avoid the electrolysis of water. Fig. 6(a–c) represents the cyclic voltammograms of Au, Pt, and Ti. Similar to Ref. [1,24], approximately symmetrical CV plots along the potential axis are observed for Pt films. However, for Au and Ti electrodes, unequal cathodic and anodic charge transfer occurs through the films and the electrolyte.

Table 2 shows the calculated CDC values of electrodes compared to that of from the literature [1,24,25]. For Pt, similar to Lee et al. [7] and Hudak et al. [2], the peaks observed at −0.5, −0.45 and 0.1 V are hydrogen desorption, adsorption, and oxygen reduction, respectively. For Au, capacitive processes and oxygen reduction are observed between −0.1 to 0.7 V and −0.5 to −0.2 V, respectively.

This behavior is identical to that of Au in 0.2 M PBS solution [26]. For Ti, between −0.6 and 0.4 V, capacitive reactions are observed. Above 0.6 V, Ti behavior is similar to Pt reported behavior in nitrogen-purged PBS using 1.0–1.5 V applied voltage [25]. Oxidation of the chloride ion and phosphate group may be the cause. This is consistent to the formation of oxide layer on electrode surfaces, which affects on the charge delivery capacity [17,18,27].

4. Conclusions

Electrochemical impedance of gold (Au), titanium (Ti), and platinum (Pt) electrodes on liquid crystal polymer (LCP) has been measured as a function of frequency and immersion time for the first time in phosphate buffered saline (PBS) solution. The electrode material changes impedance based upon frequency of application, whereby the impedance of the electrodes increases with the decrease of frequency. From experimental results, we propose the following relationship for determining impedance vs. frequency behavior:

$$|Z| = \begin{cases} f \le f_c, & \propto \dfrac{1}{f} \\ f > f_c, & \approx \text{Const.} \end{cases} \quad (3)$$

In Eq. (3), Z is the impedance, f is the application frequency of interest, and f_c is the cut-off frequency.

In the selected application frequency range, Pt shows lowest impedance followed by Ti and Au. This may be attributed to the surface roughness of electrode associated with its reactivity and capacitance in the solution in short-term evaluations. However, in order to identify such behavior in long-term, further interrogation is advised. In long-term stability, the surface roughness is severely increased after 42-days of immersion in the PBS solution. The slope of impedance decreases with elapsing time due to the degradation of the double layer capacitive behavior (i.e., β) of the electrode. The β value for Pt and Ti significantly degrades with immersion time. However, this change is not remarkable in Au.

Cyclic voltammetry investigation identifies that Pt offers highest charge delivery capacity (CDC) value followed by Au and Ti. It is clear that there is a choice between best charge transfer and long-term stability for the application frequency range. These results demonstrate Pt electrode with low electrochemical impedance and high CDC may make the best material for the short-term applications of neuromuscular electrical stimulation. Au possesses improved stability for long-term applications, albeit with higher electrochemical impedance and lower CDC. These results provide a better understanding of the electrochemical design challenges of implantable electrode for neuromuscular stimulation applications.

Acknowledgements

This research was supported by a discovery grant (Grant No. 327947) from the Natural Science and Engineering Research Council of Canada. The authors would like to thank Profs. M.J. Deen and N. Nikolova, and F. Zhang of McMaster University for their assistance.

References

[1] S.H. Lee, J.H. Jung, Y.M. Chae, J.F. Suh, J.Y. Kang, Fabrication and characterization of implantable and flexible nerve cuff electrodes with Pt, Ir and IrO_x films deposited by RF sputtering, Journal of Micromechanics and Microengineering 20 (2010), 035015 (10 pp.).
[2] E.M. Hudak, J.T. Mortimer, H.B. Martin, Platinum for neural stimulation: voltammetry considerations, Journal of Neural Engineering 7 (2010), 026005 (7 pp.).
[3] Z. Hu, D. Min Zhou, R. Greenberg, T. Thundat, Nanopowder molding method for creating implantable high-aspect-ratio electrodes on thin flexible substrates, Biomaterials 27 (2006) 2009–2017.
[4] D.R. Merrill, M. Bikson, J.G.R. Jefferys, Electrical stimulation of excitable tissue: design of efficacious and safe protocols, Journal of Neuroscience Methods 141 (2005) 171–198.
[5] D.K. Peterson, M.L. Nochomovitz, T.A. Stellato, J.T. Mortimer, Long-term intramuscular electrical activation of the phrenic nerve: efficacy as a ventilatory prosthesis, IEEE Transactions on Biomedical Engineering 41 (12) (1994) 1127–1135.
[6] D.R. Merrill, Biological and medical physics, biomedical engineering, in: D. Zhou, E. Greenbaum (Eds.), Biological and Medical Physics, Biomedical Engineering 1618–7210, Springer New York, New York, NY, 2010.
[7] I.S. Lee, C.N. Whang, J.C. Park, D.H. Lee, Biocompatibility and charge injection property of iridium film formed by ion beam assisted deposition, Biomaterials 24 (13) (2003) 2225–2231.
[8] E.T. McAdams, J. Jossinet, R. Subramanian, R.G.E. McCauley, Characterization of gold electrodes in phosphate buffered saline solution by impedance and noise measurements for biological applications, in: Proceedings of the 28th IEEE EMBS Conf., 2006, pp. 4594–4597.
[9] Y.S. Diamond, S. Krylov, T. Shmilovich, R.O. Almog, N. Fishelson, Y. Sverdlov, I. Torchinsky, G. Rosenman, A. Inberg, O. Berkh, Metallization technologies and strategies for plastic based biochips, sensors and actuators for healthcare and medical applications, ECS Transactions 23 (1) (2009) 243–254.
[10] F.J. Rodriguez, D. Ceballos, M. Schuttler, A. Valero, E. Valderrama, T. Stieglitz, X. Navarro, Polyimide cuff electrodes for peripheral nerve stimulation, Journal of Neuroscience Methods 98 (2000) 105–118.
[11] K. Takata, A. Pham, Electrical properties and practical applications of liquid crystal polymer flex, in: 6th IEEE Conf. on Polymers and Adhesives in Microelectronics and Photonics, Tokyo, 2007, pp. 67–72.
[12] S.W. Lee, J. Seo, S. Ha, E.T. Kim, H. Chung, S.J. Kim, Development of microelectrode arrays for artificial retinal implants using liquid crystal polymers, Investigative Ophthalmology & Visual Science 50 (2009) 5859–5866.
[13] K.-P. Hoffmann, R. Ruff, W. Poppendieck, Long-term characterization of electrode materials for surface electrodes in biopotential recording, in: 28th Annual International IEEE Conference of Engineering in Medicine and Biology Society (EMBS), 2006, pp. 2239–2242.
[14] J.-B. Jorcin, M.E. Orazem, N. Pebere, B. Tribollet, CPE analysis by local electrochemical impedance spectroscopy, Electrochimica Acta 51 (2006) 1473–1479.
[15] C. Fonseca, M.A. Barbos, Corrosion behaviour of titanium in biofluids containing H_2O_2 studied by electrochemical impedance spectroscopy, Corrosion Science 43 (2001) 547–559.
[16] R.M. Souto, M.M. Laz, R.L. Reis, Degradation characteristics of hydroxyapatite coatings on orthopaedic TiAlV in simulated physiological media investigated by electrochemical impedance spectroscopy, Biomaterials 24 (2003) 4213–4221.
[17] S.B. Hall, E.A. Khudaish, A.L. Hart, Electrochemical oxidation of hydrogen peroxide at platinum electrodes: part II. Effect of potential, Electrochimica Acta 43 (1998) 2015–2024.
[18] S. Andreescu, D. Andreescu, O.A. Sadik, A new electrocatalytic mechanism for the oxidation of phenols at platinum electrodes, Electrochemistry Communications 5 (8) (2003) 681–688.
[19] S. Tamilselvi, R. Murugaraj, N. Rajendran, Electrochemical impedance spectroscopic studies of titanium and its alloys in saline medium, Materials and Corrosion 58 (2007) 113–120.
[20] A.M. Fekry, M.A. Ameer, Electrochemistry and impedance studies on titanium and magnesium alloys in Ringer's solution, International Journal of Electrochemical Science 6 (2011) 1342–1354.
[21] B. Arkles, Hydrophobicity, hydrophilicity and silanes, Reprinted with permission from the October 2006 issue of Paint & Coatings Industry magazine.
[22] J. Hyun Park, N.R. Aluru, Temperature-dependent wettability on a titanium dioxide surface, Molecular Simulation 35 (2009) 31–37.
[23] J. Pan, D. Thierry, C. Leygrafi, Electrochemical and XPS studies of titanium for biomaterial applications with respect to the effect of hydrogen peroxide, Journal of Biomedial Materials Research 28 (1994) 113–122.
[24] S. Negi, R. Bhandari, L. Rieth, F. Solzbacher, In vitro comparison of sputtered iridium oxide and platinum-coated neural implantable microelectrode arrays, Biomedial Materials 5 (2010), 015007 (9 pp.).
[25] O. Niina, T. Hirotaka, K. Yoshiuki, K. Toshiya, K. Risato, T. Tetsu, H. Jari, Comparison of electrode materials for the use of retinal prosthesis, Biomedical Materials and Engineering 21 (2011) 83–97.
[26] S.E. Moultonm, J.N. Barisci, A. Bath, R. Stella, G.G. Wallace, Studies of double layer capacitance and electron transfer at a gold electrode exposed to protein solutions, Electrochemica Acta 49 (2004) 4223–4230.
[27] G. Lang, M. Ujvari, G. Inzelt, Possible origin of the deviation from the expected impedance response of polymer film electrodes, Electrochimica Acta 46 (2001) 4159–4175.

Biographies

M.M.R. Howlader received the B.Sc.Eng. degree in Electrical and Electronic Engineering from Khulna University of Engineering and Technology, Khulna, Bangladesh, in 1988, and the M.S. and Ph.D. degrees in Nuclear Engineering from Kyushu University, Fukuoka, Japan, in 1996 and 1999, respectively. Currently Dr. Howlader is leading the nanobonding and packaging research program at the Department of Electrical and Computer Engineering, McMaster University, Hamilton, ON, Canada. He has authored or coauthored more than 45-refereed papers and 70 proceedings articles. His research focuses on planar and vertical integration of

bio-micro-opto-electromechanical systems, and bioinstrumentation for health and environmental applications.

Dr. T.E. Doyle is an Assistant Professor at McMaster University and holds a Ph.D., an M.E.Sc., and a B.E.Sc in Electrical and Computer Engineering Science, and an additional B.Sc. in Computer Science. Dr. Doyle is a Professional Engineer and a member of the IEEE, ASEE, and CEEA. Research interests include Electrophysiological Sensors, Human Computer Interfacing, Embedded & Intelligent Systems, Remote and Austere Environment Medical Care and Communications. Dr. Doyle teaches courses in Engineering Design, Modeling and Simulation, and Computer Engineering.

S. Mohtashami received the B.S. degree in Biomedical Engineering from Amikabir University, Iran and the M.A.Sc. degree in Electrical and Computer Engineering, with emphasis on bio-electrochemical science from McMaster University, Canada in 2011. Currently, she is engaged in the research and development of an electrical systems design company in Ontario, Canada.

Joseph Kish received the undergraduate and graduate degree in Materials Science and Engineering from McMaster University, Hamilton, ON, Canada, in 1992 and 1999, respectively. Currently Dr. Kish is an Associate Professor at the same Department. His is engaged in the application of electrochemical techniques and high resolution microstructure characterization techniques to the study of corrosion. His current research interests include corrosion prediction and protection of structural materials in the automotive, aerospace, energy generation and chemical processing industries.